

# Discoveries in structure and physiology of mechanically activated ion channels

<https://doi.org/10.1038/s41586-020-2933-1>

J. M. Kefauver<sup>1,2,3</sup>, A. B. Ward<sup>2</sup>✉ & A. Patapoutian<sup>1</sup>✉

Received: 1 April 2020

Accepted: 19 August 2020

Published online: 25 November 2020

 Check for updates

The ability to sense physical forces is conserved across all organisms. Cells convert mechanical stimuli into electrical or chemical signals via mechanically activated ion channels. In recent years, the identification of new families of mechanosensitive ion channels—such as PIEZO and OSCA/TMEM63 channels—along with surprising insights into well-studied mechanosensitive channels have driven further developments in the mechanotransduction field. Several well-characterized mechanosensory roles such as touch, blood-pressure sensing and hearing are now linked with primary mechanotransducers. Unanticipated roles of mechanical force sensing continue to be uncovered. Furthermore, high-resolution structures representative of nearly every family of mechanically activated channel described so far have underscored their diversity while advancing our understanding of the biophysical mechanisms of pressure sensing. Here we summarize recent discoveries in the physiology and structures of known mechanically activated ion channel families and discuss their implications for understanding the mechanisms of mechanical force sensing.

From the sound of a whisper to the strike of a hammer on a finger, many familiar environmental cues occur as mechanical forces. Mechanotransduction, the conversion of mechanical perturbations into electrochemical signals, is conserved across all domains of life. It is possibly the most ancient sensory process, and may have protected early protocells from osmotic and mechanical forces that threatened to break their membranes<sup>1</sup>. The primary sensors that mediate many such rapid responses to mechanical signals are ion channels<sup>2</sup>.

Research on these channels has been impeded by their sparse expression, their need (in some cases) for specialized cellular structures and the difficulty in producing physiologically relevant mechanical stimuli that can be used across multiple cellular and experimental contexts<sup>2–5</sup>. A lack of evolutionary conservation in mechanically activated ion channels has delayed the discovery of the channels responsible for mammalian mechanotransduction in particular. In spite of these difficulties, several families of ion channels have been identified in a variety of organisms, from bacteria and flies to humans<sup>2–4</sup>. Each channel family is structurally distinct from the others, suggesting that each arose independently<sup>2–4</sup>.

Several recent advancements have prompted considerable excitement about the mechanotransduction field (also reviewed in refs.<sup>6,7</sup>). The discovery of new families of mechanically activated ion channels such as PIEZOs, which have important *in vivo* physiological roles in mammals, has opened new avenues of inquiry into the roles of mechanotransduction in human health and disease<sup>8,9</sup>. Additionally, mechanosensitive channels from the K2P (two-pore potassium) and OSCA/TMEM63 (hyperosmolality-gated calcium-permeable) channel families have been validated as bona fide mechanically activated ion channels<sup>10,11</sup>. Recent technical advances in single-particle cryo-electron microscopy (cryo-EM) have led to published structures for almost every known family of mechanically activated ion channel<sup>12–25</sup> (Fig. 1). Finally,

new insights from the best-studied mechanically activated channels have bolstered our mechanistic understanding of mechanotransduction at the molecular level<sup>13,16,26–28</sup> (Fig. 2).

## Mechanosensitive ion channel families

Ion channel families from a variety of organisms have been discovered, each with disparate structures and functions.

### MscL, MscS and MscS-like channels

The first mechanosensitive ion channels to be discovered were the prokaryotic channels mechanosensitive channel large conductance (MscL) and mechanosensitive channel small conductance (MscS), and their homologues in archaea and plants<sup>4,29–31</sup>. In bacteria, these channels respond to osmotic shock by permeating ions and osmolytes to prevent cell lysis<sup>4</sup>.

MscL is non-selective and opens its large pore like the iris of a camera in response to membrane tension<sup>32,33</sup>. Its five-subunit structure is composed of an N-terminal amphipathic helix (S1) anchored to the cytosolic leaflet followed by two transmembrane (TM) domains (TM1 and TM2) and a single cytosolic helix (S3) at the C terminus<sup>34</sup> (Fig. 1a). The pore is lined by TM1 from each subunit and the narrowest part of the pore is formed by a junction of TM1 helices near the cytoplasmic side of the membrane<sup>34</sup>. The cytosolic S3 helices form a bundle below the pore that probably acts as a selectivity filter, preventing leakage of metabolites<sup>35</sup>. Under membrane tension, the amphipathic S1 helix slides along the membrane at the lipid–solvent interface and drives a tilt in the pore-lining TM1 helix, producing an increase in pore diameter<sup>36–39</sup> (Fig. 2a). This tension-induced change in free energy overcomes the stability of the closed state, illustrating a fundamental principle in the biophysics of mechanically gated channels<sup>40,41</sup>.

<sup>1</sup>Howard Hughes Medical Institute, Department of Neuroscience, The Scripps Research Institute, La Jolla, CA, USA. <sup>2</sup>Department of Integrative Structural and Computational Biology, The Scripps Research Institute, La Jolla, CA, USA. <sup>3</sup>Present address: Department of Molecular Biology, University of Geneva, Geneva, Switzerland. ✉e-mail: andrew@scripps.edu; ardem@scripps.edu

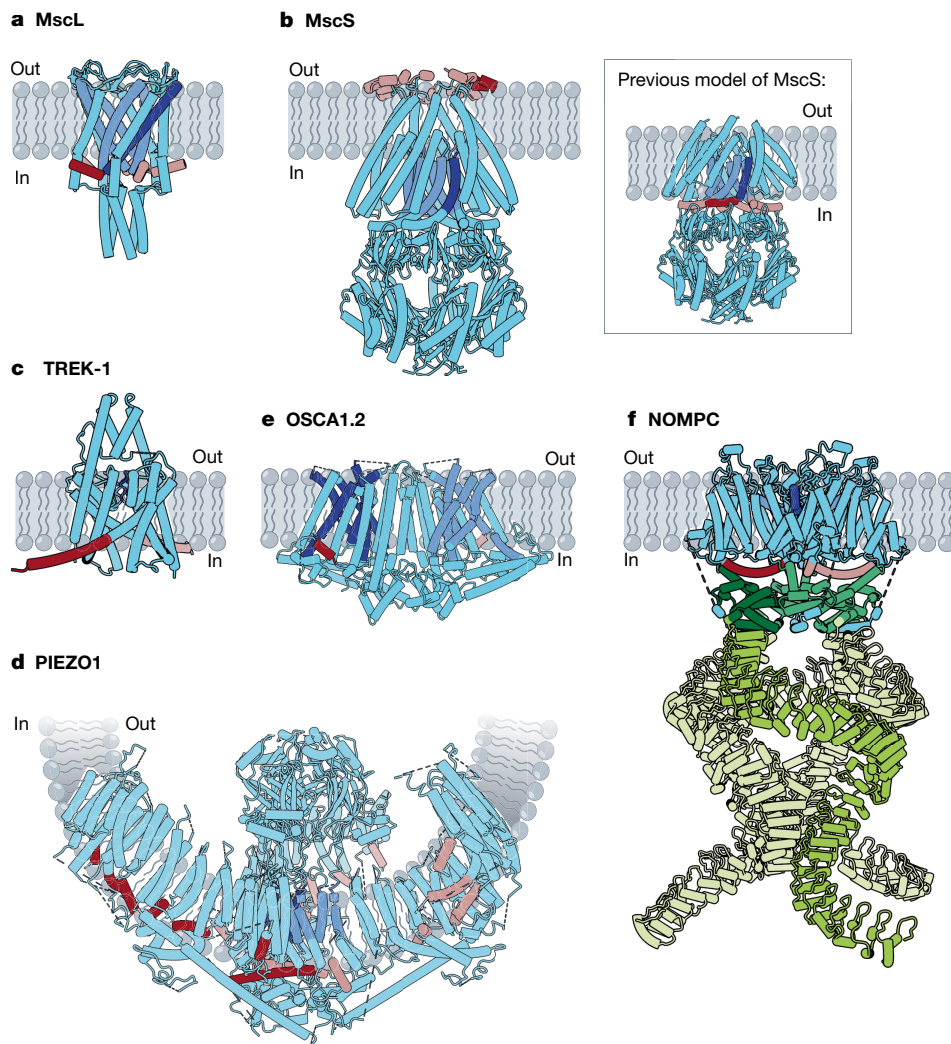


**Fig. 1 | Structures of mechanically activated ion channels.** Many mechanically activated channels seem to share a common feature: amphipathic helices (dark red on subunit A, rose on all other subunits) connected directly or indirectly to pore-lining regions (dark blue on subunit A, cornflower on all other subunits). **a**, Cartoon model of MscL (Protein Data Bank (PDB): 2OAR). Pore-lining TM1 (blue) is connected to the amphipathic S1 helix (red). **b**, Cartoon models of MscS. Main, a recent structure of MscS in nanodiscs (PDB: 6PWP), with the amphipathic anchor domain (red) sitting on the external membrane leaflet. Inset, the previous model of MscS (PDB: 2OAU), with the pore-lining TM3a helix (blue) completely embedded within the membrane and TM3b (red) predicted to be an amphipathic segment at the cytoplasmic leaflet.

MscS is structurally distinct from MscL<sup>42</sup>. It is a homo-heptamer with each protomer composed of three TM helices, with an extracellular N terminus and a cytoplasmic C terminus<sup>42</sup>. For many years, it was thought that MscS gating was analogous to that of MscL, whereby the third TM helix (TM3) served as the main pore-facing component with a cytosolic amphipathic helix (termed TM3b) formed by a kink in TM3 (Fig. 1b, insert)<sup>42–44</sup>. However, recent structures of MscS solved in lipidic nanodiscs show that this region sits below the membrane, within the cytoplasm<sup>12,13</sup> (Fig. 1b). The flexible N terminus, now designated the anchor domain, occupies the periplasmic half of the TM region and includes an amphipathic portion that sits on the periplasmic leaflet<sup>12,13</sup>. This region is important for gating by tension, and spectroscopic data suggest that it moves deeper into the membrane as the channel opens<sup>13,45,46</sup>. These structures also reveal several bound lipids that may be important for gating by mechanical stimuli<sup>12,13</sup> (Fig. 3a) and underscore the importance

**c**, Cartoon model of TREK-1 (PDB: 6CQ6). The pore domains (blue) are gated by a C-type mechanism<sup>61</sup>. The amphipathic C-tail (red) extends below the M4 helix. **d**, Cartoon model of PIEZO1 (PDB: 5Z10). Beneath the extracellular cap, two TM helices from each subunit line the pore (blue). In the domain-swapped blades, several amphipathic helices (red) line the cytoplasmic leaflet. **e**, Cartoon model of OSCA1.2 (PDB: 6MGV). Five helices (blue) line each of the two putative pores of OSCA1.2 and an amphipathic helix (red) sits on the opposite face of each subunit. **f**, Cartoon model of NOMPC (PDB: 5VK4). Each NOMPC subunit has an amphipathic TRP domain (red), a pore helix (blue) and a large spring-like ankyrin repeat domain (green).

of structural determination in lipidic environments. Another distinct feature of the MscS family is the large C-terminal cytoplasmic chamber with eight portals that open to the cytoplasm, which serves as the primary selectivity filter<sup>47,48</sup>; it may also act as a sensor of cytoplasmic crowding to prevent excessive draining of the cell<sup>49</sup> (Fig. 1b).

Homologues of MscS channels are found in plants and some fungi and protists, but not in animals<sup>50</sup>. Land plants encode several MscS-like (MSL) genes that are grouped into three categories on the basis of their subcellular localization<sup>50</sup>. MSLs in group I and group II are expressed in mitochondria and plastids, where they have an osmoregulatory role<sup>30,51</sup>. Group III MSLs reside at the plasma membrane, where their roles remain an active area of research. In *Arabidopsis thaliana*, MSL8 and MSL10 have been shown to be bona fide mechanosensitive ion channels, with roles in pollen survival<sup>52</sup>, stress-induced cell death<sup>53</sup> and cell swelling in seeds<sup>54</sup>. Recent structures of MSL1 reveal a shared architecture with

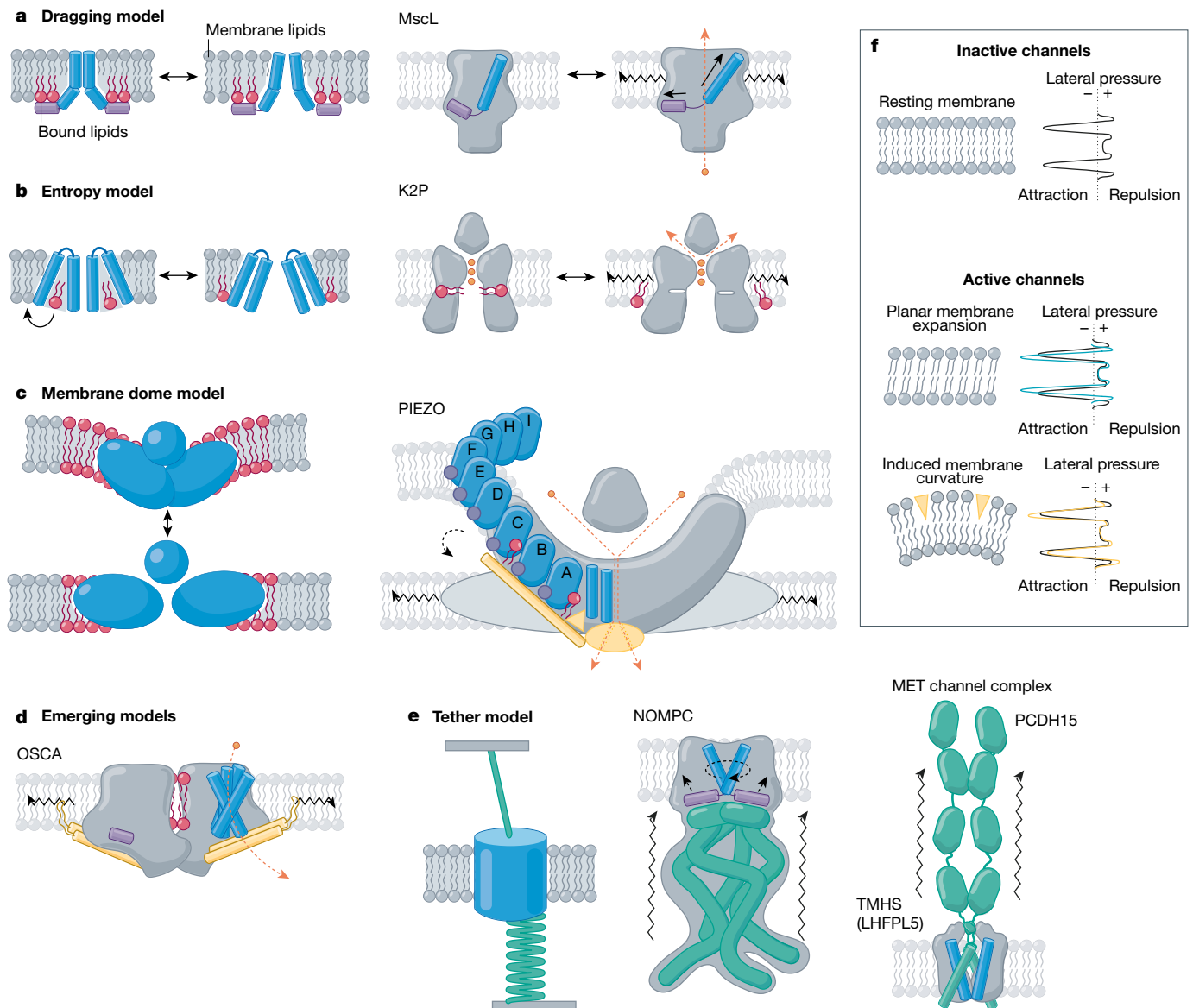


**Fig. 2 | Mechanistic models of mechanically activated ion channel gating.**

Proposed mechanistic models with channel family examples. Amphipathic helices (violet), TM helices (blue), bound lipids (red), beam-like features (gold), tethers (emerald), ions (orange) and membrane lipids (grey) are indicated. **a**, Left, the dragging model. Lipids interact with an amphipathic helix and drag it outwards upon membrane expansion<sup>4</sup>. Right, MscL, for example, has an amphipathic helix on the internal leaflet (helix S1, violet) that drives a tilt to the pore-lining helix (TM1, blue) as it is ‘dragged’ outward under tension<sup>38</sup>. **b**, Left, entropy model. Lipids reside in hydrophobic pockets in the closed state and exit these pockets under membrane tension, inducing a conformational change<sup>132</sup>. Right, K2P, for example, has a fenestration occupied by lipid acyl tails (red) when inactive, whereas in active channels, this fenestration is closed and lipids are absent. **c**, Left, membrane dome model. Channel curvature within the membrane stores energy<sup>18</sup>. Right, PIEZOs, for example, expand and flatten<sup>134</sup>, gating the pore via interactions between the beam domain, the anchor domain and the CTD (gold)<sup>90</sup>. **d**, Emerging models. OSCA channels have lipid-occupied pores and an

intersubunit cleft (red), an amphipathic helix (violet) on the inner leaflet, and a beam-like domain (gold) connected to pore-lining helices, which terminates a membrane-entrant hook domain (gold); all of these domains could have a role in gating<sup>23</sup>. **e**, Left, the tether model. Force is transmitted to the channel via a tether to the extracellular matrix, the cytoskeleton or both. For example, NOMPC (middle) is tethered to microtubules via its ankyrin repeat domain (emerald)<sup>112</sup>. Right, the MET channel complex is tethered to the neighbouring stereocilium via the tip link (PCDH15; emerald)<sup>16</sup>. **f**, Top, resting membrane tension. The transbilayer pressure profile reflects the lateral pressure experienced through the bilayer as a consequence of repulsion (positive pressure) of the lipid head groups, attraction (negative pressure) due to surface tension at the glycerol backbone, and steric hindrance (positive pressure) between the lipid tails<sup>32</sup>. Bottom, model membranes under tension. Planar membrane expansion thins the bilayer and increases the area occupied by each lipid. Membrane curvature is induced when suction is applied to the membrane or conical-shaped amphipathic compounds insert into the bilayer<sup>130,148</sup>.

MscS, although two additional TM domains present in MSL1 sit at an angle within the membrane to create a bowl-shaped TM region that is dilated and flattened in open structures of the channel<sup>55,56</sup>.

### Two-pore potassium channels

Three members of the two-pore potassium channel (K2P) family are inherently mechanosensitive ion channels: TREK-1, TREK-2 and TRAAK<sup>10</sup>.

TRAAK and TREK channels can be activated by a variety of mechanical stimuli, including stretching, poking, swelling and fluid jet stimulation, as well as temperature and a diverse group of chemicals, including lysolipids, volatile anaesthetics and antidepressants<sup>57</sup>. Both TRAAK and TREK channels are sensitive to a wide range of tension, from 0.5 mN m<sup>-1</sup> to the membrane lytic point of 12 mN m<sup>-1</sup>, and their open probabilities are proportional to the applied membrane tension<sup>57</sup>. Although these



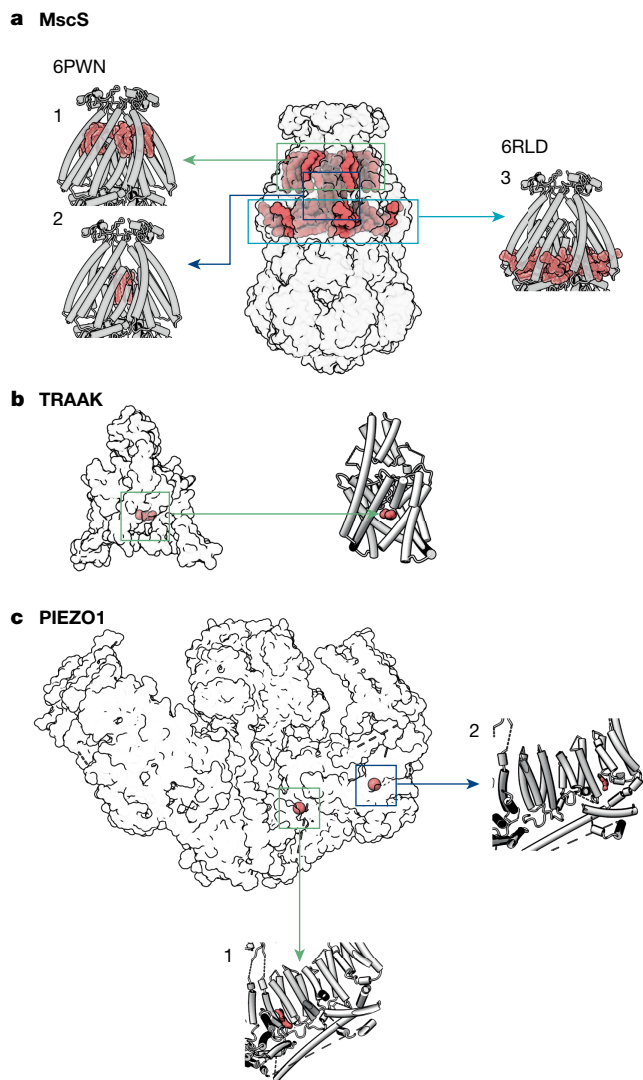


**Fig. 3 | Lipids observed in structures of mechanosensitive ion channels.**

**a**, Lipids are observed in three locations in MscS structures. (1) One lipid per subunit is 'hooked' at the periplasmic leaflet<sup>12,13</sup>; (2) densities ascribed to lipid acyl chains reside inside the pore<sup>12,13</sup> (PDB: 6PWN). (3) Two additional lipids per protomer are observed parallel to TM3b, below the membrane leaflet<sup>12</sup> (PDB: 6RLD). **b**, In inactive structures of TRAAK (PDB: 4WWF), an acyl tail (green) occupies a fenestration below the selectivity filter<sup>62</sup>. **c**, Two lipid-like densities are observed in the PIEZO1 structure (PDB: 6BPZ): (1) in the region between the anchor domain and piezo repeat A, and (2) between piezo repeats B and C (second and third from the pore, respectively)<sup>19</sup>.

channels are expressed in sensory neurons, they are not involved in generating action potentials; instead, they dampen the transduction currents of a non-selective cationic mechanosensor by hyperpolarizing cells<sup>10</sup>. Knockout mice with deletions of each of these three genes exhibit hypersensitivity to mechanical stimuli<sup>57</sup>. A recent study using monoclonal antibodies specific to TRAAK showed that it is not localized at nerve terminals (where sensory transduction initiates), but is instead present exclusively in the nodes of Ranvier in myelinated neurons<sup>58</sup>. This raises the possibility that one of its roles is to prevent misfiring in the event of neuronal stretch, or perhaps compensate the mechanical force induced by an action potential<sup>58</sup>. However, because these ion channels respond to a variety of activators, a role of mechanical forces in the nodes of Ranvier cannot yet be attributed with certainty.

K2Ps have two concatenated pore-facing domains per subunit, which dimerize to form a pseudotetramer with two final amphipathic

C-terminal tails<sup>59</sup> (Fig. 1c). In contrast to many K<sup>+</sup> channels, K2Ps rely on a C-type gating mechanism<sup>60</sup>. In C-type gating, the mobility of residues in the selectivity filter determines whether ions are able to permeate the channel<sup>60</sup>. In crystal structures of TREKs and TRAAK, two main conformations are observed: a 'down' state in which a fenestration below the selectivity filter opens towards the membrane, and an 'up' state in which the final TM helix (M4) bends upward to occlude this opening<sup>27,61–63</sup> (Fig. 2b). Assigning a functional state to these conformations has been difficult, but evidence from studies with the state-dependent blocker norfluoxetine indicate that, for mechanical activation at least, the up state is most probably the active state of the channel<sup>27,64,65</sup>.

Several mechanisms of mechanosensitivity for K2P channels have been proposed. The first is similar to that of MscL, in which an increased cross-sectional area of the protein is more energetically favourable under membrane tension<sup>40,41</sup>. Because the selectivity filters of TREK and TRAAK channels must maintain structural integrity to retain selectivity for potassium ions, only the portion of the channel below the selectivity filter (in the cytoplasmic leaflet of the membrane) expands in-plane under tension<sup>65,66</sup>. An alternative mechanism has been suggested on the basis of the observation that in structures of the presumptive inactive down state, lipids or detergent molecules occupy the fenestration below the selectivity filter<sup>62,67</sup>, but this lipid binding site is occluded in the presumptive active up state, suggesting that bound lipids have a role in gating<sup>62,65</sup> (Figs. 2b, 3b). How these conformational changes affect the C-type gate remains unknown.

### PIEZO1 and PIEZO2

The PIEZO family is conserved from protozoa to humans and was the first identified class of non-selective cationic mechanotransducers shown to be physiologically relevant in mammals<sup>9</sup>. Relative to other known channel families, PIEZOs have roles in a broad and varied set of mechanotransduction processes<sup>3,9</sup>. PIEZOs are involved in well-characterized mechanosensory roles such as touch<sup>9</sup>, mechanical allodynia (a clinically relevant form of pain)<sup>68,69</sup> and the baroreceptor reflex<sup>70</sup>, as well as several unexpected functions, including developmental processes (such as lymphatic valve development<sup>71,72</sup>, heart valve development<sup>73,74</sup>, angiogenesis<sup>75</sup> and stem cell differentiation<sup>76</sup>) and regulatory processes (such as bone formation<sup>77,78</sup>, cell migration<sup>79</sup>, axon regeneration<sup>80</sup>, the inflammatory response of innate immune cells<sup>81</sup> and red blood cell (RBC) volume regulation<sup>82</sup>). Additionally, one-third of the human population of African descent harbours a relatively mild gain-of-function mutation in *PIEZO1* that causes RBC dehydration (consistent with hereditary xerocytosis) and confers resistance to malaria<sup>82,83</sup>.

PIEZO1 and PIEZO2 are large trimeric proteins with a triskelion or three-blade propeller architecture<sup>18–21,84</sup>. The three blade domains extend outward within the lipid bilayer and an extracellular cap domain resides above the central pore<sup>18–21</sup> (Fig. 1d). The cap domain appears to have a major role in channel inactivation<sup>85–87</sup>. PIEZOs have an unusually large number of TM passes per protomer; 38 TM helices per subunit are resolved in the PIEZO2 structure<sup>21</sup>, matching previous membrane topology predictions for PIEZO1<sup>88</sup>. The first 36 TM helices that form the flexible blades of PIEZO assemble into nine repeating elements of four-helix bundles preceded by an N-terminal amphipathic helix, termed Piezo repeats<sup>18–21</sup> (Fig. 2c). Notably, amphipathic helices are known to sense and/or induce membrane curvature<sup>9,89</sup>. The Piezo repeats spiral away from the centre of the channel in a helical conformation, resulting in an overall puckered architecture of the channel<sup>18–21,84</sup> (Fig. 1d). The curved form of PIEZOs could cause a local distortion to the native cell membrane or result in its preferred localization to a membrane domain of similar curvature<sup>18–21</sup>. While it is possible that detergent solubilization of PIEZOs alters its native conformation<sup>19,21</sup>, when purified PIEZO1 is reconstituted into lipid vesicles, the protein deforms the vesicle, producing a similar curvature to that observed in the detergent-solubilized structures<sup>18</sup>. Furthermore, interactions that occur between the cap



domain and the blades in the curved conformation are important for PIEZO1 inactivation, suggesting that this architecture represents the closed or inactivated state of PIEZOs<sup>18,87</sup>.

The pore of PIEZO is lined by the final two C-terminal TM helices, termed the inner and outer helices<sup>18–21,84</sup>. The central pore and the domain-swapped extracellular cap resemble the architecture of P2X channels and acid-sensing ion channels (ASICs), but the C-terminal domain (CTD), the anchor domain and the large blades are unique to PIEZOs<sup>18</sup>. PIEZO structures provide clues regarding how these three features might contribute to mechanosensitivity. The intracellular CTDs form a vestibule with three portals that are probably a continuation of the ion conduction pathway<sup>20,90</sup>. Juxtaposed against the CTD, the wedge-shaped anchor domain is inserted into the inner leaflet of the membrane, lodged between the pore-lining helix pair and the nearest piezo repeat (piezo repeat A)<sup>18–21,84</sup> (Fig. 2c). Beneath each blade, a long beam-like helix extends under the first three piezo repeats (piezo repeats A–C), then hinges at a conserved motif<sup>18–20</sup>. The beam terminates near the central pore, just below the CTD<sup>18–21,84</sup> (Figs. 1d, 2c). One possibility for mechanical gating is that movements of the beam can be transmitted to the pore by a network of interactions between the CTD, the anchor domain and the pore-lining helices<sup>19,20,90–92</sup>. Because the blades are also domain-swapped relative to the inner or outer helix pair, a flattening or lever-like motion in the blades could produce a lateral dilation or unraveling of the CTD region via its interactions with the beam<sup>20,90–92</sup>.

Despite the large size of PIEZO proteins, relatively few pharmacological tools have been found to modulate their activity. PIEZO1 and PIEZO2 can both be inhibited by the tarantula toxin GsMTx4<sup>93,94</sup>; however, this amphipathic peptide toxin is suggested to interact with the membrane, relieving the effects of tension in the outer bilayer leaflet rather than binding specifically to PIEZOs<sup>95</sup>. The small molecule Yoda1 can activate PIEZO1, but not PIEZO2<sup>96</sup>. An additional small molecule, Dooku1, acts as an antagonist of Yoda1 with no agonist capability<sup>97</sup>. PIEZO1 probably harbours a specific binding site for Yoda1 in the region between the anchor domain and piezo repeat A<sup>98</sup>. Of note, a lipid density is observed between these two domains in cryo-EM structures, along with an additional lipid density between piezo repeats B and C<sup>19</sup> (Fig. 3c).

### OSCA/TMEM63 channels

OSCA/TMEM63 proteins constitute the largest family of mechanosensitive channels<sup>99</sup>. Initially described as hyperosmolarity sensors in *A. thaliana*, OSCA proteins have recently been shown to be pore-forming, inherently mechanosensitive channels that are conserved across plants and animals<sup>11,100</sup>. OSCAs and their mechanosensitive animal homologues TMEM63A and TMEM63B are stretch-activated at a high threshold relative to PIEZO channels<sup>11,22</sup>. In plants, mutations in OSCA1.1 impair guard cell responses to stress and inhibit root growth under hyperosmotic conditions<sup>100</sup>. In humans, mutations in TMEM63A are associated with a myelination defect in infants<sup>101</sup>, although it is currently unclear whether this is related to a mechanosensory role.

Several structures of different OSCA family members in detergent and lipidic nanodiscs have been solved by cryo-EM<sup>22–25</sup>. These dimeric channels have two pores and 11 TM helices per subunit<sup>22–25</sup> (Fig. 1e). They are predicted to share structural homology with the TMEM16 family of ion channels or scramblases, as well as potentially transmembrane channel-like protein 1 (TMCL1), which is involved in hereditary deafness (see below), on the basis of modelling and mutagenesis studies<sup>23,25,102,103</sup>. Multiple structural features have been identified that might confer mechanosensitivity to these channels (Fig. 2d). One is the hydrophobic cleft at the dimeric interface that is occupied by lipid molecules in molecular dynamics simulations<sup>23,24</sup> (Fig. 2d). Flexibility between the two protomers may allow an increase in cross-sectional area in response to membrane tension<sup>23</sup>. A hydrophobic groove in the cytosolic pore vestibule opens towards the membrane<sup>22–24</sup>, similar to the fenestration observed in mechanosensitive K2Ps. In molecular dynamics

simulations, this region is occupied by lipids<sup>23</sup>. Upon membrane stretch, lipids residing in the cytosolic pore vestibules or the hydrophobic cleft could unbind or dissociate. One of the pore-lining helices (TM6) also lines this fenestration and is bent at a glycine residue that, in a manner analogous to gating in MscL, might straighten during channel activation<sup>22,24,26</sup>. At its C terminus, TM6 interacts with a distinct feature of OSCAs—a cytosolic domain composed of two parallel helices connected by a membrane-anchored loop<sup>22–25</sup> (Fig. 2d). This beam-like domain is predicted to be one of the most dynamic regions of the channel<sup>24,25</sup>. It may act as a stretch sensor that coordinates the movements of the TM helices, similar to a model for PIEZO mechanosensing<sup>90,91</sup>. Experimental data to support these possibilities is lacking at the moment, and an understanding of gating will require structure–function analysis as well as structures of the open state.

### Transient receptor potential channels

Transient receptor potential (TRP) channels are involved in a variety of sensory processes including chemosensation, thermosensation, mechanosensation and osmosensation, often exhibiting polymodal gating by chemicals, signalling lipids (for example, phosphatidylinositol-4,5-bisphosphate (PtdIns(4,5)P<sub>2</sub>)), and physical stimuli<sup>104</sup>. They all share a canonical tetrameric architecture, with cytosolic N and C termini and six TM domains<sup>104</sup>. Several members of the TRP ion channel family have been proposed to be mechanosensitive<sup>2</sup>. However, with the exception of the *Drosophila melanogaster* mechanosensor, no mechanoreceptor potential C (NOMPC)<sup>105,106</sup>, proving that TRP channels are directly activated by mechanical stimuli has been difficult.

*nompC* was first cloned from fruit fly sensory bristles<sup>105</sup>. It is selectively expressed in the ciliated mechanosensory organs of *D. melanogaster*, *Caenorhabditis elegans*<sup>105</sup> and zebrafish<sup>107</sup> at locations where mechanical forces impinge on the sensory cilia<sup>108</sup>. NOMPC is a bona fide mechanically activated ion channel in *Drosophila*, but it has no mammalian homologues<sup>109</sup>. The N terminus of NOMPC contains a cytosolic 29-ankyrin repeat domain (ARD), which is required for microtubule association, proper localization and the in vivo function of NOMPC<sup>106</sup>. This ARD can be observed by transmission electron microscopy as a filament that is able to adopt variable lengths (20–80 nm) connecting the membrane to microtubules in *Drosophila* campaniform mechanoreceptors<sup>110</sup>.

A cryo-EM structure revealed that the ARDs of NOMPC form a flexible helical bundle with several intersubunit interactions<sup>14</sup> (Fig. 1f). Atomic force microscopy measurements had previously shown that isolated NOMPC ARD acts analogously to a linear and fully reversible spring<sup>111</sup>. Molecular dynamics simulations using the NOMPC structure show that compression of the ARDs can produce a clockwise movement of the TRP domain and linker helices, similar to the TRPV1 closed-to-open gating transition<sup>28,112</sup> (Fig. 2e). The data are consistent with the tether model of mechanotransduction, in which the ARD of NOMPC acts as a spring that transduces the movement of the microtubules relative to the membrane into channel gating.

The most compelling case for direct mechanical activation of a mammalian TRP channel has been made for TRPV4<sup>113</sup>. TRPV4 has been implicated in several processes that may rely on mechanosensitive ion channels, including osmoregulation, control of vascular tone and nociception<sup>15,113</sup>. Mechanically activated currents induced by a pilus-deflection stimulus in mouse primary chondrocytes are dependent on TRPV4, and heterologous expression of TRPV4 in hamster embryonic kidney cells also induces these currents<sup>113</sup>. However, like all other tested mammalian TRP channels, TRPV4 is not activated by stretch, suggesting that mammalian TRPs are not inherently mechanosensitive<sup>113,114</sup>. Tethering of TRPV4 to the extracellular matrix (ECM), the cytoskeleton or some other localized factor is postulated to enable TRPV4 mechanosensitivity<sup>113</sup>. Another possibility is that TRPV4 responds to a downstream signal initiated by a primary mechanotransducer, such as the amphipathic molecule diacylglycerol<sup>114</sup>. Cryo-EM and X-ray diffraction

## Review

structures of TRPV4 provide few clues as to what structural features may contribute to its putative gating by mechanical stimuli<sup>15</sup>.

### Mechano-electrical transduction channel complex

The first measurement of mechanically activated currents was in mechanosensory hair cells of the auditory and vestibular systems that sense vibrations induced by pressure waves at specialized hair bundle structures called stereocilia<sup>115,116</sup>. The stereocilia are arranged in a staircase pattern of rows of similar height and are connected by filamentous tip links (Fig. 4a). When the stereocilia are deflected, the tip links are thought to transmit force to a mechanically gated ion channel, resulting in depolarization of the hair cell<sup>116</sup>. The exquisite structural complexity of the mechanosensory hair cells has impeded the decades-long search for the mechano-electrical transduction (MET) channel complex that underlies this current<sup>116</sup>. Several proteins have been identified that are essential to MET<sup>116</sup>. The tip link is a tether composed of two components: cadherin 23 is attached to the upper stereocilium and protocadherin 15 (PCDH15) is connected to a lower stereocilium where the MET channel is localized<sup>116</sup> (Fig. 4b). Three candidate proteins are essential for MET channel currents and colocalize with PCDH15: (1) TMC1 or TMC2, (2) transmembrane inner ear (TMIE), and (3) lipoma high mobility group IC fusion partner-like (LHFPL5) (also called tetraspan membrane protein of hair cell stereocilia (TMHS))<sup>116</sup> (Fig. 4b).

Several recent studies support the contribution of TMC1 and TMC2 to the MET channel pore. First, a mutation in TMC1 that causes deafness in mice (called Beethoven (*Bth*)) also alters ion permeability, single channel conductance and channel blockade of MET channel currents<sup>103</sup>. Additionally, a structural model of TMC1 based on its loose homology to the TMEM16 protein family predicts a dimeric two-pore structure with a membrane-facing groove<sup>102,103</sup>. Cysteine-scanning mutagenesis has identified residues that contribute to the pore pathway on each of four pore-lining helices predicted by the homology model<sup>102</sup>. Finally, reconstitution of purified TMC1 from green sea turtles and TMC2 from budgerigars into liposomes is reported to enable the measurement of pressure-sensitive currents, providing the strongest evidence to date that TMCs are mechanically activated ion channels<sup>117</sup>. Replication of this result, especially with vertebrate channels, would be ideal given the non-conserved function of several other mechanically activated channel families. While it is likely that TMC1 contributes to the MET channel pore, it remains unclear whether it is the only molecule that underlies MET currents in all types of hair cells. For example, knockout of LHFPL5 has also been shown to affect conductance and adaptation properties of mechanically activated currents in hair cells<sup>118</sup>, and mutations in the C-terminal lipid-binding domain of TMIE also alter conductance as well as ion selectivity<sup>119</sup>.

It has been difficult to obtain atomic-resolution structures of many MET channel components, possibly because their stability is dependent on the intricate structure of the hair cells<sup>16,116</sup>. However, a structural approach in which the entire multi-protein MET channel complex is reconstituted for cryo-EM single-particle analysis may be transformative for the field<sup>16</sup>. This work has been initiated with a structure of truncated PCDH15 co-expressed with LHFPL5, revealing the interactions between these components at subnanometer resolution<sup>16</sup> (Fig. 4c). LHFPL5 is a dimeric complex of 4-TM-helix protomers; where the two protomers meet, they form a V-shaped interface that is lined by TM1 of each protomer. Each of the two PCDH15 proteins contributes a single TM pass that forms an inverted V shape that inserts into and interacts with the TM1 helices of LHFPL5<sup>16</sup> (Figs. 2e, 4c). Because the two PCDH15 protomers are connected by a stable linker domain, force along the tip link would probably pull the PCDH15 TM helices apart, transmitting force to LHFPL5<sup>16</sup>.

### Degenerin, epithelial sodium channels and ASICs

The degenerin (DEG) family of ion channels (named for the cell swelling and neurodegeneration phenotype these proteins cause)

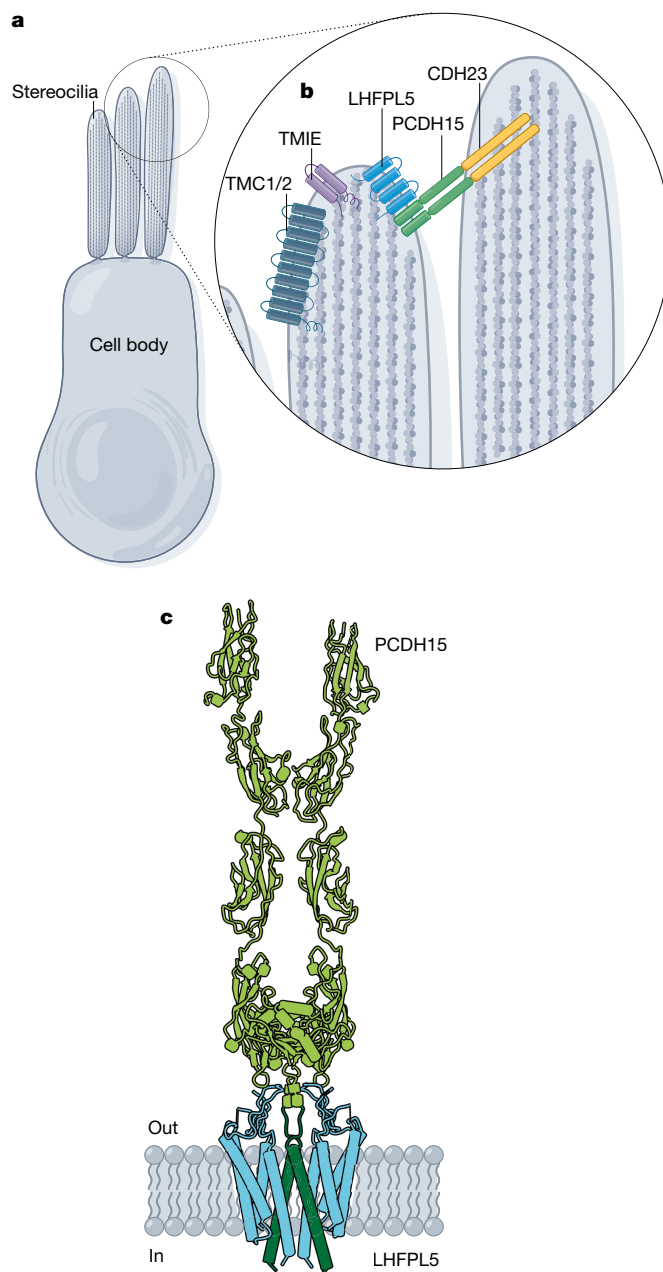


**Fig. 4 | The MET channel complex.** **a**, Model of a hair cell. **b**, MET channel complex components: TMC1 or TMC2, TMIE and LHFPL5 are localized to the stereocilia tips. Tip links are formed by dimers of PCDH15 and cadherin 23 (CDH23). **c**, Cartoon model of components of the MET channel complex: PCDH15 forms the lower half of the tip link (green) and LHFPL5 is a dimeric TM protein (blue) (PDB: 6C13 and 6C14).

was first discovered through a genetic screen of touch-insensitive *C. elegans* mutants<sup>120</sup>. MEC-4, a founding member of the DEG family, is a pore-forming subunit of the ion channel responsible for mechanosensitive currents in the gentle touch receptors of worms<sup>2</sup>. It assembles as a channel that can also include the protein MEC-10<sup>2,121</sup>. Several additional *C. elegans* proteins are also important for mechanosensation, although they are not channel proteins. MEC-2 (homologous to stomatin-like protein 3 (STOML3) in mammals) and MEC-6 enhance mechanosensitive channel activity, probably by modifying the cholesterol content of the membrane<sup>2,121</sup>. An additional set of ECM-associated proteins, MEC-1 and MEC-9, are proposed to contribute to an extracellular tether that connects MEC-4–MEC-10 channels to the ECM<sup>2</sup>. In mammals, two

channel families, epithelial sodium channels (ENaCs) and ASICs, share homology with the *C. elegans* MEC-4–MEC-10 channels<sup>2</sup>. Roles for these channels in mechanosensory processes such as blood pressure sensing and nociception have been described, but there is a lack of evidence that these channels are directly activated by mechanical stimuli<sup>122,123</sup>. A recent study revealed that two glycosylated asparagines in ENaC probably serve as a tether to the ECM, building on the idea that this channel family might sense tension via a filament tether<sup>124</sup>.

## Mechanistic insights

With the discovery of disparate families of mechanosensitive ion channels and the subsequent structural and biophysical insights, our mechanistic understanding of mechanotransduction is developing rapidly. Two classic models for transmitting force to an ion channel remain in the spotlight: the force-from-lipids model and the force-from-tether model. We also discuss a third, hybrid model whereby modulation by both lipids and cytoskeleton can have a role.

### The force-from-lipids model

The force-from-lipids model involves the direct conversion of tension in the membrane to area expansion in mechanosensitive proteins, without the need for additional elements such as cytoskeleton or accessory proteins<sup>125</sup>. An ion channel is considered ‘inherently mechanosensitive’ if it can be mechanically activated after purification and reconstitution in a lipid bilayer<sup>126</sup>. MscL<sup>32,127</sup>, MscS<sup>127</sup>, TRAAK<sup>10</sup>, TREK-1<sup>10</sup>, PIEZO1<sup>128</sup> and several OSCA family members<sup>11</sup> all meet this standard. This mechanistic conservation is unsurprising, as membrane-embedded protein domains exist in the context of the chemical and biophysical properties of the bilayer, enabling sensitivity to tension in the bilayer.

At rest, all membrane-embedded proteins experience a mix of hydrophobic and steric forces exerted by the bilayer lipids, termed the ‘transbilayer pressure profile’<sup>126,129</sup> (Fig. 2f). When the bilayer stretches, the membrane thins and the local transbilayer pressure profile changes<sup>126,129</sup>. Mechanically activated ion channels change conformation in response to hydrophobic mismatch between their membrane-facing domains and the bilayer, producing gating movements to open the pore<sup>126,129,130</sup>.

Another way to conceptualize the effect of membrane tension is as an increase in the planar area of the bilayer lipids, shifting the equilibrium such that hydrophobic forces that tend to cluster lipids overcome the forces that mediate protein–lipid interactions<sup>65,131,132</sup>. In this ‘entropy-driven’ model, lipids that stabilize the closed state of the protein dissociate, resulting in a conformational change to compensate the unoccupied hydrophobic pockets<sup>131,132</sup> (Fig. 2b). For example, in structures of the two-pore potassium channels, TRAAK and TREK-1, membrane lipids bound to a fenestration below the channel pore stabilize the closed conformation of the channel; in structures of open channels, those lipids are absent<sup>62</sup>. Lipids are predicted to occupy similar pore-adjacent fenestrations of several different channels including MscL<sup>38</sup>, MscS<sup>12,13</sup>, MSL1 and OSCA1.2<sup>23–24</sup>, as well as near the pore region in structures of PIEZO1<sup>19,98</sup>.

An alternative model suggests that bound lipids maintain their interactions with the protein rather than dissociating under tension. This ‘dragging’ model, based on observations of MscL, proposes that lipids do work on an amphipathic helix connected to a pore lining helix, straightening it as the membrane equilibrates under tension<sup>4,26</sup> (Fig. 2a). Amphipathic helices are present in MscL<sup>26,34</sup>, MscS<sup>13</sup>, TRAAK and TREK<sup>27,62,63</sup>, PIEZOs<sup>19–21</sup> and OSCA1.2<sup>23–25</sup>, although a direct connection to a pore-lining segment is only present in the case of MscL<sup>36,37</sup> (Fig. 2a). For PIEZOs and OSCAs, a link between the amphipathic helices and the pore is possible via a more complex network of allosteric interactions<sup>13,19,20,22–24</sup> (Fig. 2c, d). Alternatively, the membrane-anchored loop of the beam-like domain of OSCA might substitute an amphipathic helix to serve a similar dragging function (Fig. 2d).

A different type of membrane distortion is a change in curvature<sup>32</sup> (Fig. 2c). Channel activity of MscL, MscS, TREK-1, PIEZO1 and OSCA1 can all be modulated by the addition of conical lipids or amphipathic molecules that tend to bend membranes<sup>22,126</sup>. As membrane curvature can gate mechanically activated channels, the intrinsic curvature of PIEZOs is notable. A ‘dome mechanism’ has been proposed for PIEZO activation, in which its large size and curved shape enable a large increase of in-plane area as PIEZO flattens under tension<sup>18,133,134</sup> (Fig. 2c). Bolstering this model, PIEZO1 protein reconstituted in planar membranes undergoes substantial area expansion when tension is applied to the membrane by an atomic force microscopy cantilever<sup>134</sup>. Moreover, the bending force that the curvature of PIEZO would exert on the membrane is predicted to extend past the edge of the protein into the bilayer to create a ‘membrane footprint’<sup>133</sup>. A similar membrane dome mechanism has recently been proposed for MSL1<sup>56</sup>.

### Tethering to ECM or cytoskeleton

The alternative mechanism is one in which mechanosensitive proteins are tethered to the ECM, the cytoskeleton, or both ECM and cytoskeleton, enabling forces experienced by these cellular compartments to be transmitted to these ion channels via a connecting structure. The *Drosophila* channel NOMPC, with its spring-like ankyrin repeats<sup>14,28,110</sup>, and the MET channel complex, with its tip links, are clear examples of tethered channels<sup>16</sup> (Fig. 2e). The involvement of tether molecules has also been proposed for somatosensory touch function<sup>135</sup>. Within the DEG–ENAC–ASIC superfamily, ENaC and probably MEC-4–MEC-10 channels also function via a tether to the ECM<sup>2,124</sup>, and TRPV4 and other TRP channels may also use such a tether<sup>113,114</sup>.

### Mechanisms of modulation

There is evidence that these two models are not mutually exclusive<sup>136</sup>. For example, the conspicuously tethered channel NOMPC also responds to force-from-lipids activation<sup>4,14</sup>. A NOMPC residue that interacts with lipid head groups is, in fact, essential for mechanical activation of the channel<sup>4,14</sup>. Conversely, effects of the cytoskeleton, regulatory proteins and signalling lipids have also been observed for inherently mechanosensitive channels.

PIEZO1 and TREK-1 activity can be modulated in complex ways by the presence of cytoskeletal elements<sup>9,137</sup>. For instance, the application of cytochalasin D, which disrupts the actin cytoskeleton, positively modulates PIEZO1 under some circumstances and negatively modulates it in others<sup>9</sup>. Another important modulatory factor for mechanosensitive proteins is the composition of the membrane in which they are embedded. TREK1 and TRAAK are activated by the signalling lipid PtdIns(4,5)P<sub>2</sub><sup>138</sup>, and depletion of PtdIns(4,5)P<sub>2</sub> and PtdIns(4)P inhibit PIEZO1 and PIEZO2<sup>139</sup>.

Lipid rafts and other membrane lipid subdomains may also be important for mechanotransduction. An interesting theory suggests that mechanotransduction occurs at ‘force foci’, specific cholesterol- and sphingolipid-rich membrane subdomains localized to adherens junctions and focal adhesions<sup>140</sup>. A study that followed raft-localized phospholipase D signalling after mechanical stimulation demonstrates that mechanical force is capable of disrupting cholesterol-rich rafts<sup>141</sup>. A membrane-subdomain model is compatible with tethered multi-protein assemblies such as the MET channel complex, but recent studies suggest that it may also be relevant to PIEZOs; PIEZO1 appears to localize to focal adhesions in glioma cells<sup>142</sup>. Additionally, in a subset of mechanoreceptive neurons, co-expression of PIEZO1 with cytoskeleton-associated STOML3 lowers the activation threshold of the channel by an order of magnitude<sup>143,144</sup>. STOML3 functions by binding cholesterol and forming a membrane-associated scaffold in a manner that resembles putative force foci<sup>143,144</sup>.

As our ability to study membrane proteins in their native context improves, we may discover that the regulation of mechanosensitive proteins by membrane lipids is far more complex and intricate than individual channel structures have so far revealed.



## Outlook

The explosion of new structural models of mechanosensitive ion channels provides an excellent starting point for structure–function studies and molecular dynamics simulations to develop increasingly refined models of mechanotransduction. However, for many channel families, particularly those in vertebrates, these efforts are hindered by the absence of structures of open channels. Producing a mechanical stimulus suitable for structural studies is a substantial challenge, as high-resolution structure determination currently requires purification and isolation away from the membrane. Chemical agonists that could trap an open state have been difficult to identify for channels such as PIEZO1 and PIEZO2<sup>96</sup>. For channel complexes such as the MET channel, purification and reconstitution of a complete set of proteins necessary for channel function is a formidable technical challenge<sup>16</sup>. As cryo-electron tomography and correlated light and electron microscopy improve, the ability to acquire high-resolution structures in situ might provide a new view of mechanically activated channels in native membranes.

Despite the substantial recent progress in identification and characterization of mechanically activated ion channels, a variety of biological processes that depend on mechanotransduction remain poorly understood at the molecular level, and the identities of many mechanosensors remain elusive, including that of the sensor(s) for mammalian acute pain. Further characterization of the physiological roles of PIEZOs and the OSCA/TMEM63 family in animals and plants may provide some of these answers, but the search for unknown mechanosensors remains imperative. Indeed, two new families of mechanically activated ion channels, TACAN<sup>145</sup> and Elkin<sup>146</sup>, have recently been proposed. It may also prove valuable to broaden the search for mechanosensing molecules beyond ion channels, as mechanical stimuli also affect development and growth processes that do not depend on neuronal action potentials. For example, the G-protein-coupled receptor GPR68 was recently shown to be activated by shear stress to release intracellular calcium stores, regulating blood vessel dilation<sup>147</sup>. It will be important for these initial findings on proposed mechanosensitive ion channels and G-protein-coupled receptors to be replicated by other groups in the field, and we hope that future structural and physiological studies will extend these initial observations.

Finally, the identification of new families of mechanically activated channels will expand our knowledge on the role of mechanotransduction in previously unrecognized areas of physiology and disease. By using expression patterns of newly identified mechanosensors as a starting point, loss-of-function and gain-of-function mutations can be powerful genetic tools to gain in-depth insights into the in vivo consequences of sensing mechanical force. Furthermore, probing human genetic data for mutations in mechanosensors will be instrumental in defining their roles in human disease. Indeed, recent discoveries on the role of PIEZO1 in bone formation, RBC hydration and immune function in humans and in mice are examples of how genetic studies on mechanosensors can lead to mechanistic understanding of the role of pressure sensing in unexpected areas of biology and disease<sup>77,78,81,82</sup>.

- Anishkin, A., Loukin, S. H., Teng, J. & Kung, C. Feeling the hidden mechanical forces in lipid bilayer is an original sense. *Proc. Natl Acad. Sci. USA* **111**, 7898–7905 (2014).
  - Arnadóttir, J. & Chalfie, M. Eukaryotic mechanosensitive channels. *Annu. Rev. Biophys.* **39**, 111–137 (2010).
  - Ranade, S. S., Syeda, R. & Patapoutian, A. Mechanically activated ion channels. *Neuron* **87**, 1162–1179 (2015).
  - Cox, C. D., Bavi, N. & Martinac, B. Bacterial mechanosensors. *Annu. Rev. Physiol.* **80**, 71–93 (2018).
  - Chalfie, M. Neurosensory mechanotransduction. *Nat. Rev. Mol. Cell Biol.* **10**, 44–52 (2009).
  - Douguet, D. & Honoré, E. Mammalian mechano-electrical transduction: structure and function of force-gated ion channels. *Cell* **179**, 340–354 (2019).
  - Jin, P., Jan, L. Y. & Jan, Y.-N. Mechanosensitive ion channels: structural features relevant to mechanotransduction mechanisms. *Annu. Rev. Neurosci.* **43**, 207–229 (2020).
  - Coste, B. et al. Piezo1 and Piezo2 are essential components of distinct mechanically activated cation channels. *Science* **330**, 55–60 (2010).
- This study uses an RNA interference screen to identify PIEZOs as essential components of a mechanically activated ion channel.**

- Murthy, S. E., Dubin, A. E. & Patapoutian, A. Piezos thrive under pressure: mechanically activated ion channels in health and disease. *Nat. Rev. Mol. Cell Biol.* **18**, 771–783 (2017).
  - Brohawn, S. G., Su, Z. & MacKinnon, R. Mechanosensitivity is mediated directly by the lipid membrane in TRAAK and TREK1 K<sup>+</sup> channels. *Proc. Natl Acad. Sci. USA* **111**, 3614–3619 (2014).
- This study demonstrates that the mechanically activated K2P channels, TRAAK and TREK1, are inherently mechanosensitive.**
- Murthy, S. E. et al. OSCA/TMEM63 are an evolutionarily conserved family of mechanically activated ion channels. *eLife* **7**, 1–17 (2018).
- Several OSCA genes and their mammalian homologues, the TMEM63 family, are shown to be inherently mechanosensitive ion channels.**
- Rasmussen, T., Flegler, V. J., Rasmussen, A. & Böttcher, B. Structure of the mechanosensitive channel MscS embedded in the membrane bilayer. *J. Mol. Biol.* **431**, 3081–3090 (2019).
  - Reddy, B., Bavi, N., Lu, A., Park, Y. & Perozo, E. Molecular basis of force-from-lipids gating in the mechanosensitive channel MscS. *eLife* **8**, e50486 (2019).
- These two articles present cryo-EM structures of the bacterial MscS channel in a lipidic nanodisc, substantially updating our understanding of how it is embedded within the membrane.**
- Jin, P. et al. Electron cryo-microscopy structure of the mechanotransduction channel NOMPC. *Nature* **547**, 118–122 (2017).
- This study presents the cryo-EM structure of NOMPC, revealing that the large ankyrin repeat domain is arranged with a large spring-like architecture.**
- Deng, Z. et al. Cryo-EM and X-ray structures of TRPV4 reveal insight into ion permeation and gating mechanisms. *Nat. Struct. Mol. Biol.* **25**, 252–260 (2018).
  - Ge, J. et al. Structure of mouse protocadherin 15 of the stereocilia tip link in complex with LHFPL5. *eLife* **7**, e38770 (2018).
- Co-expression and purification of the MET complex components PCDH15 and LHFPL5 reveal that a TM helix of the PCDH15 subunit interacts extensively with the TM helices of each LHFPL5 subunit.**
- Noreng, S., Bharadwaj, A., Posert, R., Yoshioka, C. & Bacongus, I. Structure of the human epithelial sodium channel by cryo-electron microscopy. *eLife* **7**, e39340 (2018).
  - Guo, Y. R. & MacKinnon, R. Structure-based membrane dome mechanism for Piezo mechanosensitivity. *eLife* **6**, e33660 (2017).
  - Saotome, K. et al. Structure of the mechanically activated ion channel Piezo1. *Nature* **554**, 481–486 (2018).
  - Zhao, Q. et al. Structure and mechanogating mechanism of the Piezo1 channel. *Nature* **554**, 487–492 (2018).
  - Wang, L. et al. Structure and mechanogating of the mammalian tactile channel PIEZO2. *Nature* **573**, 225–229 (2019).
- These four studies present cryo-EM structures of PIEZO1 and PIEZO2, revealing that its curved shape probably resides within the membrane, and providing a near-atomic-resolution view of several features that may be involved in gating by mechanical force.**
- Zhang, M. et al. Structure of the mechanosensitive OSCA channels. *Nat. Struct. Mol. Biol.* **25**, 850–858 (2018).
  - Jojoa-Cruz, S. et al. Cryo-EM structure of the mechanically activated ion channel OSCA1.2. *eLife* **7**, e41845 (2018).
  - Liu, X., Wang, J. & Sun, L. Structure of the hyperosmolality-gated calcium-permeable channel OSCA1.2. *Nat. Commun.* **9**, 5060 (2018).
  - Maitly, K. et al. Cryo-EM structure of OSCA1.2 from *Oryza sativa* elucidates the mechanical basis of potential membrane hyperosmolality gating. *Proc. Natl Acad. Sci. USA* **116**, 14309–14318 (2019).
- These four studies present cryo-EM structures of OSCA1.2 and other OSCA family members, revealing their structural homology to TMEM16 and highlighting features that may be involved in mechanical gating.**
- Bavi, N., Cox, C. D., Perozo, E. & Martinac, B. Toward a structural blueprint for bilayer-mediated channel mechanosensitivity. *Channels* **11**, 91–93 (2017).
- This study proposed the dragging mechanism of mechanotransduction.**
- Dong, Y. Y. et al. K2P channel gating mechanisms revealed by structures of TREK-2 and a complex with Prozac. *Science* **347**, 1256–1259 (2015).
  - Argudo, D., Capponi, S., Bethel, N. P. & Grabe, M. A multiscale model of mechanotransduction by the ankyrin chains of the NOMPC channel. *J. Gen. Physiol.* **151**, 316–327 (2019).
  - Sukharev, S. I., Martinac, B., Arshavsky, V. Y. & Kung, C. Two types of mechanosensitive channels in the *Escherichia coli* cell envelope: solubilization and functional reconstitution. *Biophys. J.* **65**, 177–183 (1993).
  - Haswell, E. S. & Meyerowitz, E. M. MscS-like proteins control plastid size and shape in *Arabidopsis thaliana*. *Curr. Biol.* **16**, 1–11 (2006).
  - Kloda, A. & Martinac, B. Common evolutionary origins of mechanosensitive ion channels in Archaea, Bacteria and cell-walled Eukarya. *Archaea* **1**, 35–44 (2002).
  - Perozo, E., Kloda, A., Cortes, D. M. & Martinac, B. Physical principles underlying the transduction of bilayer deformation forces during mechanosensitive channel gating. *Nat. Struct. Mol. Biol.* **9**, 696–703 (2002).
  - Betanzos, M., Chiang, C. S., Guy, H. R. & Sukharev, S. A large iris-like expansion of a mechanosensitive channel protein induced by membrane tension. *Nat. Struct. Biol.* **9**, 704–710 (2002).
- Disulfide cross-linking between the first TM helices on adjacent subunits of MscL in the resting state and in osmotically shocked cells provides the first evidence for the area-expansion model of mechanotransduction.**
- Chang, G., Spencer, R. H., Lee, A. T., Barclay, M. T. & Rees, D. C. Structure of the MscL homolog from *Mycobacterium tuberculosis*: a gated mechanosensitive ion channel. *Science* **282**, 2220–2226 (1998).
  - Anishkin, A. et al. On the conformation of the COOH-terminal domain of the large mechanosensitive channel MscL. *J. Gen. Physiol.* **121**, 227–244 (2003).
  - Islcia, I., Wray, R. & Blount, P. The dynamics of protein–protein interactions between domains of MscL at the cytoplasmic–lipid interface. *Channels* **6**, 255–261 (2012).

37. Li, J. et al. Mechanical coupling of the multiple structural elements of the large-conductance mechanosensitive channel during expansion. *Proc. Natl Acad. Sci. USA* **112**, 10726–10731 (2015).
38. Bavi, N. et al. The role of MscL amphipathic N terminus indicates a blueprint for bilayer-mediated gating of mechanosensitive channels. *Nat. Commun.* **7**, 11984 (2016).
39. Wang, Y. et al. Single molecule FRET reveals pore size and opening mechanism of a mechano-sensitive ion channel. *eLife* **3**, e01834 (2014).
40. Chiang, C. S., Anishkin, A. & Sukharev, S. Gating of the large mechanosensitive channel in situ: estimation of the spatial scale of the transition from channel population responses. *Biophys. J.* **86**, 2846–2861 (2004).
41. Wiggins, P. & Phillips, R. Membrane–protein interactions in mechanosensitive channels. *Biophys. J.* **88**, 880–902 (2005).
42. Bass, R. B., Strop, P., Barclay, M. & Rees, D. C. Crystal structure of *Escherichia coli* MscS, a voltage-modulated and mechanosensitive channel. *Science* **298**, 1582–1587 (2002).
43. Wang, W. et al. The structure of an open form of an *E. coli* mechanosensitive channel at 3.45 Å resolution. *Science* **321**, 1179–1183 (2008).
44. Anishkin, A., Kamaraju, K. & Sukharev, S. Mechanosensitive channel MscS in the open state: modeling of the transition, explicit simulations, and experimental measurements of conductance. *J. Gen. Physiol.* **132**, 67–83 (2008).
45. Vásquez, V., Sotomayor, M., Cordero-Morales, J., Schulten, K. & Perozo, E. A structural mechanism for MscS gating in lipid bilayers. *Science* **321**, 1210–1214 (2008).
46. Rasmussen, T. et al. Interaction of the mechanosensitive channel, MscS, with the membrane bilayer through lipid intercalation into grooves and pockets. *J. Mol. Biol.* **431**, 3339–3352 (2019).
47. Edwards, M. D., Bartlett, W. & Booth, I. R. Pore mutations of the *Escherichia coli* MscS channel affect desensitization but not ionic preference. *Biophys. J.* **94**, 3003–3013 (2008).
48. Cox, C. D. et al. Selectivity mechanism of the mechanosensitive channel MscS revealed by probing channel subconducting states. *Nat. Commun.* **4**, 2137 (2013).
49. Rowe, I., Anishkin, A., Kamaraju, K., Yoshimura, K. & Sukharev, S. The cytoplasmic cage domain of the mechanosensitive channel MscS is a sensor of macromolecular crowding. *J. Gen. Physiol.* **143**, 543–557 (2014).
50. Hamilton, E. S., Schlegel, A. M. & Haswell, E. S. United in diversity: mechanosensitive ion channels in plants. *Annu. Rev. Plant Biol.* **66**, 113–137 (2015).
51. Lee, J. S., Wilson, M. E., Richardson, R. A. & Haswell, E. S. Genetic and physical interactions between the organellar mechanosensitive ion channel homologs MSL1, MSL2, and MSL3 reveal a role for inter-organellar communication in plant development. *Plant Direct* **3**, e00124 (2019).
52. Hamilton, E. S. & Haswell, E. S. The tension-sensitive ion transport activity of MSL8 is critical for its function in pollen hydration and germination. *Plant Cell Physiol.* **58**, 1222–1237 (2017).
53. Basu, D., Shoots, J. M. & Haswell, E. S. Interactions between the N- and C-termini of the mechanosensitive ion channel ATMSL10 are consistent with a three-step mechanism for activation. *J. Exp. Bot.* **71**, 4020–4032 (2020).
54. Basu, D. & Haswell, E. S. The mechanosensitive ion channel MSL10 potentiates responses to cell swelling in *Arabidopsis* seedlings. *Curr. Biol.* **30**, 2716–2728.e6 (2020).
55. Li, Y. et al. Structural insights into a plant mechanosensitive ion channel MSL1. *Cell Rep.* **30**, 4518–4527.e3 (2020).
- This study presents the open and closed structures of MSL1, providing insights into the gating of this plant mechanosensitive channel.**
56. Deng, Z. et al. Structural mechanism for gating of a eukaryotic mechanosensitive channel of small conductance. *Nat. Commun.* **11**, 3690 (2020).
57. Brohawn, S. G. How ion channels sense mechanical force: insights from mechanosensitive K2P channels TRAAK, TREK1, and TREK2. *Ann. NY Acad. Sci.* **1352**, 20–32 (2015).
58. Brohawn, S. G. et al. The mechanosensitive ion channel TRAAK is localized to the mammalian node of Ranvier. *eLife* **8**, 713990 (2019).
59. Brohawn, S. G., Campbell, E. B. & MacKinnon, R. Domain-swapped chain connectivity and gated membrane access in a Fab-mediated crystal of the human TRAAK K<sup>+</sup> channel. *Proc. Natl Acad. Sci. USA* **110**, 2129–2134 (2013).
60. Schewe, M. et al. A non-canonical voltage-sensing mechanism controls gating in K2P K<sup>+</sup> channels. *Cell* **164**, 937–949 (2016).
61. Brohawn, S. G., del Mármol, J. & MacKinnon, R. Crystal structure of the human K2P TRAAK, a lipid- and mechano-sensitive K<sup>+</sup> ion channel. *Science* **335**, 436–441 (2012).
62. Brohawn, S. G., Campbell, E. B. & MacKinnon, R. Physical mechanism for gating and mechanosensitivity of the human TRAAK K<sup>+</sup> channel. *Nature* **516**, 126–130 (2014).
63. Lolicato, M., Riegelhaupt, P. M., Arrigoni, C., Clark, K. A. & Minor, D. L., Jr. Transmembrane helix straightening and buckling underlies activation of mechanosensitive and thermosensitive K(2P) channels. *Neuron* **84**, 1198–1212 (2014).
- These two articles present crystal structures of mechanosensitive K2P channels with opposing interpretations of the activity state of the channel; Brohawn et al. observe lipid density that extends into the channel pore.**
64. McClenaghan, C. et al. Polymodal activation of the TREK-2 K2P channel produces structurally distinct open states. *J. Gen. Physiol.* **147**, 497–505 (2016).
65. Aryal, P. et al. Bilayer-mediated structural transitions control mechanosensitivity of the TREK-2 K2P channel. *Structure* **25**, 708–718.e2 (2017).
- Molecular dynamics modelling of TREK-2 elucidates the gating transition upon membrane tension.**
66. Clausen, M. V., Jarerattanachai, V., Carpenter, E. P., Sansom, M. S. P. & Tucker, S. J. Asymmetric mechanosensitivity in a eukaryotic ion channel. *Proc. Natl Acad. Sci. USA* **114**, E8343–E8351 (2017).
67. Lolicato, M. et al. K<sub>2P</sub>2.1 (TREK-1)-activator complexes reveal a cryptic selectivity filter binding site. *Nature* **547**, 364–368 (2017).
68. Murthy, S. E. et al. The mechanosensitive ion channel Piezo2 mediates sensitivity to mechanical pain in mice. *Sci. Transl. Med.* **10**, eaat9897 (2018).
69. Szczot, M. et al. PIEZO2 mediates injury-induced tactile pain in mice and humans. *Sci. Transl. Med.* **10**, eaat9892 (2018).
70. Zeng, W. Z. et al. PIEZO2 mediates neuronal sensing of blood pressure and the baroreceptor reflex. *Science* **362**, 464–467 (2018).
71. Nonomura, K. et al. Mechanically activated ion channel PIEZO1 is required for lymphatic valve formation. *Proc. Natl Acad. Sci. USA* **115**, 12817–12822 (2018).
72. Choi, D. et al. Piezo1 incorporates mechanical force signals into the genetic program that governs lymphatic valve development and maintenance. *JCI Insight* **4**, e125068 (2019).
73. Faucherre, A. et al. Piezo1 is required for outflow tract and aortic valve development. *J. Mol. Cell. Cardiol.* **143**, 51–62 (2020).
74. Duchemin, A. L., Vignes, H. & Vermot, J. Mechanically activated piezo channels modulate outflow tract valve development through the Yap1 and Klf2–Notch signaling axis. *eLife* **8**, e44706 (2019).
75. Kang, H. et al. Piezo1 mediates angiogenesis through activation of MT1-MMP signaling. *Am. J. Physiol. Cell Physiol.* **316**, C92–C103 (2019).
76. He, L., Si, G., Huang, J., Samuel, A. D. T. & Perrimon, N. Mechanical regulation of stem-cell differentiation by the stretch-activated Piezo channel. *Nature* **555**, 103–106 (2018).
77. Sun, W. et al. The mechanosensitive Piezo1 channel is required for bone formation. *eLife* **8**, e47454 (2019).
78. Li, X. et al. Stimulation of Piezo1 by mechanical signals promotes bone anabolism. *eLife* **8**, e49631 (2019).
79. Ellefsen, K. L. et al. Myosin-II mediated traction forces evoke localized Piezo1-dependent Ca<sup>2+</sup> flickers. *Commun. Biol.* **2**, 298 (2019).
80. Song, Y. et al. The mechanosensitive ion channel Piezo inhibits axon regeneration. *Neuron* **102**, 373–389 (2019).
81. Solis, A. G. et al. Mechanosensation of cyclical force by PIEZO1 is essential for innate immunity. *Nature* **573**, 69–74 (2019).
82. Ma, S. et al. Common PIEZO1 allele in African populations causes RBC dehydration and attenuates *Plasmodium* infection. *Cell* **173**, 443–455 (2018).
83. Nguetse, C. N. et al. A common polymorphism in the druggable ion channel PIEZO1 is associated with protection from severe malaria. *Proc. Natl Acad. Sci. USA* **117**, 9074–9081 (2020).
84. Ge, J. et al. Architecture of the mammalian mechanosensitive Piezo1 channel. *Nature* **527**, 64–69 (2015).
85. Wu, J., Goyal, R. & Grandl, J. Localized force application reveals mechanically sensitive domains of Piezo1. *Nat. Commun.* **7**, 12939 (2016).
86. Wu, J. et al. Inactivation of mechanically activated Piezo1 ion channels is determined by the C-terminal extracellular domain and the inner pore helix. *Cell Rep.* **21**, 2357–2366 (2017).
87. Lewis, A. H. & Grandl, J. Inactivation kinetics and mechanical gating of Piezo1 ion channels depend on subdomains within the cap. *Cell Rep.* **30**, 870–880 (2020).
88. Coste, B. et al. Piezo1 ion channel pore properties are dictated by C-terminal region. *Nat. Commun.* **6**, 7223 (2015).
89. Drin, G. & Antony, B. Amphipathic helices and membrane curvature. *FEBS Lett.* **584**, 1840–1847 (2010).
90. Geng, J. et al. A plug-and-latch mechanism for gating the mechanosensitive Piezo channel. *Neuron* **106**, 438–451 (2020).
91. Wang, Y. et al. A lever-like transduction pathway for long-distance chemical- and mechano-gating of the mechanosensitive Piezo1 channel. *Nat. Commun.* **9**, 1300 (2018).
92. Taberner, F. J. et al. Structure-guided examination of the mechanogating mechanism of PIEZO2. *Proc. Natl Acad. Sci. USA* **116**, 14260–14269 (2019).
93. Bae, C., Sachs, F. & Gottlieb, P. A. The mechanosensitive ion channel Piezo1 is inhibited by the peptide GsMTx4. *Biochemistry* **50**, 6295–6300 (2011).
94. Alcaïno, C., Knutson, K., Gottlieb, P. A., Farrugia, G. & Beyder, A. Mechanosensitive ion channel Piezo2 is inhibited by D-GsMTx4. *Channels* **11**, 245–253 (2017).
95. Suchyna, T. M. Piezo channels and GsMTx4: two milestones in our understanding of excitatory mechanosensitive channels and their role in pathology. *Prog. Biophys. Mol. Biol.* **130**, 244–253 (2017).
96. Syeda, R. et al. Chemical activation of the mechanotransduction channel Piezo1. *eLife* **4**, e07369 (2015).
97. Evans, E. L. et al. Yoda1 analogue (Dooku1) which antagonizes Yoda1-evoked activation of Piezo1 and aortic relaxation. *Br. J. Pharmacol.* **175**, 1744–1759 (2018).
98. Lacroix, J. J., Botello-Smith, W. M. & Luo, Y. Probing the gating mechanism of the mechanosensitive channel Piezo1 with the small molecule Yoda1. *Nat. Commun.* **9**, 2029 (2018).
99. Hou, C. et al. DUF221 proteins are a family of osmosensitive calcium-permeable cation channels conserved across eukaryotes. *Cell Res.* **24**, 632–635 (2014).
100. Yuan, F. et al. OSCA1 mediates osmotic-stress-evoked Ca<sup>2+</sup> increases vital for osmosensing in *Arabidopsis*. *Nature* **514**, 367–371 (2014).
101. Yan, H. et al. Heterozygous variants in the mechanosensitive ion channel TMEM63A result in transient hypomyelination during infancy. *Am. J. Hum. Genet.* **105**, 996–1004 (2019).
102. Pan, B. et al. TMC1 forms the pore of mechanosensory transduction channels in vertebrate inner ear hair cells. *Neuron* **99**, 736–753 (2018).
103. Ballesteros, A., Fenollar-Ferrer, C. & Swartz, K. J. Structural relationship between the putative hair cell mechanotransduction channel TMC1 and TMEM16 proteins. *eLife* **7**, e38433 (2018).
104. Startek, J. B., Boonen, B., Talavera, K. & Meseguer, V. TRP channels as sensors of chemically-induced changes in cell membrane mechanical properties. *Int. J. Mol. Sci.* **20**, 371 (2019).
105. Walker, R. G., Willingham, A. T. & Zuker, C. S. A. A *Drosophila* mechanosensory transduction channel. *Science* **287**, 2229–2234 (2000).
- This study identifies the nompC gene via a genetic screen with a readout of transduction currents upon mechanical stimulus of mechanoreceptor bristles in *D. melanogaster*.**
106. Cheng, L. E., Song, W., Looger, L. L., Jan, L. Y. & Jan, Y. N. The role of the TRP channel NompC in *Drosophila* larval and adult locomotion. *Neuron* **67**, 373–380 (2010).
107. Sidi, S., Friedrich, R. W. & Nicolson, T. NompC TRP channel required for vertebrate sensory hair cell mechanotransduction. *Science* **301**, 96–99 (2003).
108. Lee, J., Moon, S., Cha, Y. & Chung, Y. D. *Drosophila* TRPN(NOMP) channel localizes to the distal end of mechanosensory cilia. *PLoS ONE* **5**, e11012 (2010).

109. Yan, Z. et al. *Drosophila* NOMPC is a mechanotransduction channel subunit for gentle-touch sensation. *Nature* **493**, 221–225 (2013).
110. Sun, L. et al. Ultrastructural organization of NompC in the mechanoreceptive organelle of *Drosophila* campaniform mechanoreceptors. *Proc. Natl Acad. Sci. USA* **116**, 7343–7352 (2019).
111. Lee, G. et al. Nanospring behaviour of ankyrin repeats. *Nature* **440**, 246–249 (2006).
112. Wang, Y. et al. Push-to-open: The gating mechanism of the tethered mechanosensitive ion channel NompC. Preprint at <https://doi.org/10.1101/853721> (2019).
113. Servin-Vences, M. R., Moroni, M., Lewin, G. R. & Poole, K. Direct measurement of TRPV4 and PIEZO1 activity reveals multiple mechanotransduction pathways in chondrocytes. *eLife* **6**, e21074 (2017).
114. Nikolaev, Y. A. et al. Mammalian TRP ion channels are insensitive to membrane stretch. *J. Cell Sci.* **132**, 238360 (2019).
115. Corey, D. P. & Hudspeth, A. J. Kinetics of the receptor current in bullfrog saccular hair cells. *J. Neurosci.* **3**, 962–976 (1983).
- This study provided one of the first confirmations of the existence of a channel directly activated by mechanical stimuli, measured in hair cells from the vestibular system of a bullfrog.**
116. Cunningham, C. L. & Müller, U. Molecular structure of the hair cell mechano-electrical transduction complex. *Cold Spring Harb. Perspect. Med.* **9**, a033167 (2019).
117. Jia, Y. et al. TMC1 and TMC2 proteins are pore-forming subunits of mechanosensitive ion channels. *Neuron* **105**, 310–321 (2020).
- A study showing that TMC1 and TMC2 proteins, putative pore-forming components of the MET channel complex, form mechanically activated channels when reconstituted in liposomes.**
118. Xiong, W. et al. TMHS is an integral component of the mechanotransduction machinery of cochlear hair cells. *Cell* **151**, 1283–1295 (2012).
119. Cunningham, C. L. et al. TMIE defines pore and gating properties of the mechanotransduction channel of mammalian cochlear hair cells. *Neuron* **107**, 126–143 (2020).
120. Driscoll, M. & Chalfie, M. The *mec-4* gene is a member of a family of *Caenorhabditis elegans* genes that can mutate to induce neuronal degeneration. *Nature* **349**, 588–593 (1991).
- In this study, *mec-4*, the founding member of the DEG gene family of mechanoreceptors in *C. elegans*, was cloned.**
121. Chen, Y., Bharill, S., Isacoff, E. Y. & Chalfie, M. Subunit composition of a DEG/ENaC mechanosensory channel of *Caenorhabditis elegans*. *Proc. Natl Acad. Sci. USA* **112**, 11690–11695 (2015).
122. Ben-Shahar, Y. Sensory functions for degenerin/epithelial sodium channels (DEG/ENaC). *Adv. Genet.* **76**, 1–26 (2011).
123. Lin, S. H. et al. Evidence for the involvement of ASIC3 in sensory mechanotransduction in proprioceptors. *Nat. Commun.* **7**, 11460 (2016).
124. Knoepp, F. et al. Shear force sensing of epithelial Na<sup>+</sup> channel (ENaC) relies on N-glycosylated asparagines in the palm and knuckle domains of  $\alpha$ ENaC. *Proc. Natl Acad. Sci. USA* **117**, 717–726 (2020).
125. Martinac, B., Adler, J. & Kung, C. Mechanosensitive ion channels of *E. coli* activated by amphipaths. *Nature* **348**, 261–263 (1990).
126. Martinac, B. et al. Tuning ion channel mechanosensitivity by asymmetry of the transbilayer pressure profile. *Biophys. Rev.* **10**, 1377–1384 (2018).
127. Nomura, T. et al. Differential effects of lipids and lyso-lipids on the mechanosensitivity of the mechanosensitive channels MscL and MscS. *Proc. Natl Acad. Sci. USA* **109**, 8770–8775 (2012).
128. Syeda, R. et al. Piezo1 channels are inherently mechanosensitive. *Cell Rep.* **17**, 1739–1746 (2016).
129. Cantor, R. S. The influence of membrane lateral pressures on simple geometric models of protein conformational equilibria. *Chem. Phys. Lipids* **101**, 45–56 (1999).
130. Ridone, P. et al. “Force-from-lipids” gating of mechanosensitive channels modulated by PUFAs. *J. Mech. Behav. Biomed. Mater.* **79**, 158–167 (2018).
131. Pliotas, C. et al. The role of lipids in mechanosensation. *Nat. Struct. Mol. Biol.* **22**, 991–998 (2015).
132. Pliotas, C. & Naismith, J. H. Spectator no more, the role of the membrane in regulating ion channel function. *Curr. Opin. Struct. Biol.* **45**, 59–66 (2017).
- This review discusses an entropy-based mechanism of mechanotransduction in which lipids dissociate from hydrophobic pockets, inducing conformational changes in mechanically-activated channels.**
133. Haselwandter, C. A. & MacKinnon, R. Piezo’s membrane footprint and its contribution to mechanosensitivity. *eLife* **7**, e41968 (2018).
134. Lin, Y.-C. C. et al. Force-induced conformational changes in PIEZO1. *Nature* **573**, 230–234 (2019).
- This study uses atomic force microscopy to both induce membrane tension and measure its effects on reconstituted PIEZO1, providing evidence that PIEZO1 expands under tension.**
135. Hu, J., Chiang, L. Y., Koch, M. & Lewin, G. R. Evidence for a protein tether involved in somatic touch. *EMBO J.* **29**, 855–867 (2010).
136. Cox, C. D., Bavi, N. & Martinac, B. Biophysical principles of ion-channel-mediated mechanosensory transduction. *Cell Rep.* **29**, 1–12 (2019).
137. Li Fraine, S., Patel, A., Duprat, F. & Sharif-Naeini, R. Dynamic regulation of TREK1 gating by polycystin 2 via a filamin A-mediated cytoskeletal mechanism. *Sci. Rep.* **7**, 17403 (2017).
138. Lopes, C. M. B. et al. PIP2 hydrolysis underlies agonist-induced inhibition and regulates voltage gating of two-pore domain K<sup>+</sup> channels. *J. Physiol.* **564**, 117–129 (2005).
139. Borbiri, I., Badheka, D. & Rohacs, T. Activation of TRPV1 channels inhibits mechanosensitive Piezo channel activity by depleting membrane phosphoinositides. *Sci. Signal.* **8**, ra15 (2015).
140. Anishkin, A. & Kung, C. Stiffened lipid platforms at molecular force foci. *Proc. Natl Acad. Sci. USA* **110**, 4886–4892 (2013).
- This article proposes an innovative model for mechanotransduction in which cholesterol-rich platforms, maintained by cholesterol-binding scaffold proteins and localized to focal adhesions or adherens junctions, provide specialized force-sensing domains.**
141. Petersen, E. N., Chung, H. W., Nayebosadri, A. & Hansen, S. B. Kinetic disruption of lipid rafts is a mechanosensor for phospholipase D. *Nat. Commun.* **7**, 13873 (2016).
142. Chen, X. et al. A feedforward mechanism mediated by mechanosensitive ion channel PIEZO1 and tissue mechanics promotes glioma aggression. *Neuron* **100**, 799–815 (2018).
143. Poole, K., Herget, R., Lapatsina, L., Ngo, H. D. & Lewin, G. R. Tuning Piezo ion channels to detect molecular-scale movements relevant for fine touch. *Nat. Commun.* **5**, 3520 (2014).
144. Qi, Y. et al. Membrane stiffening by STOML3 facilitates mechanosensation in sensory neurons. *Nat. Commun.* **6**, 8512 (2015).
145. Beaulieu-Laroche, L. et al. TACAN is an ion channel involved in sensing mechanical pain. *Cell* **180**, 956–967 (2020).
146. Patkunarajah, A. et al. TMEM87a/Elkin1, a component of a novel mechano-electrical transduction pathway, modulates melanoma adhesion and migration. *eLife* **9**, e53308 (2020).
147. Xu, J. et al. GPR68 senses flow and is essential for vascular physiology. *Cell* **173**, 762–775 (2018).
148. Bavi, O., Vossoughi, M., Naghdabadi, R. & Jamali, Y. The combined effect of hydrophobic mismatch and bilayer local bending on the regulation of mechanosensitive ion channels. *PLoS ONE* **11**, e0150578 (2016).

**Acknowledgements** This work was supported by NIH grants R01 HL143297. A.P. is an investigator of the Howard Hughes Medical Institute. We thank J. Grandl, S. Murthy, S. Jojoa-Cruz and A. Gharpure for critical reading of the manuscript.

**Author contributions** J.M.K., A.B.W. and A.P. conceptualized the content of this work. J.M.K. reviewed the literature and drafted the manuscript and figures. J.M.K., A.B.W. and A.P. discussed, wrote and edited the Review.

**Competing interests** The authors declare no competing interests.

#### Additional information

**Correspondence and requests for materials** should be addressed to A.B.W. or A.P.

**Peer review information** *Nature* thanks Boris Martinac and the other, anonymous, reviewer(s) for their contribution to the peer review of this work.

**Reprints and permissions information** is available at <http://www.nature.com/reprints>.

**Publisher’s note** Springer Nature remains neutral with regard to jurisdictional claims in published maps and institutional affiliations.

© Springer Nature Limited 2020